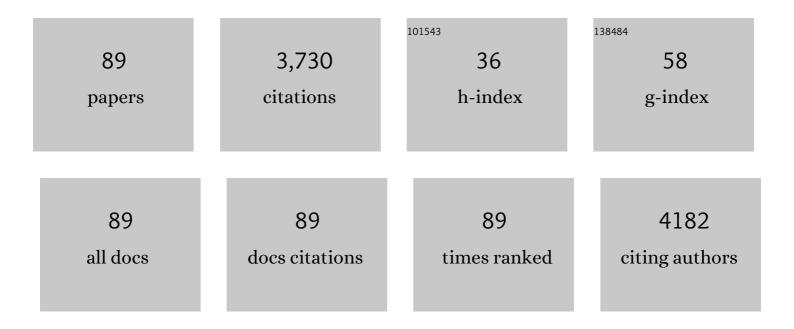
List of Publications by Year in descending order

Source: https://exaly.com/author-pdf/6855223/publications.pdf Version: 2024-02-01



YIYONG LI

#	Article	IF	CITATIONS
1	Adsorption of Cu2+, Cd2+ and Ni2+ from aqueous single metal solutions on graphene oxide membranes. Journal of Hazardous Materials, 2015, 297, 251-260.	12.4	295
2	Research progress on distribution, migration, transformation of antibiotics and antibiotic resistance genes (ARGs) in aquatic environment. Critical Reviews in Biotechnology, 2018, 38, 1195-1208.	9.0	169
3	Shape effect on the antibacterial activity of silver nanoparticles synthesized via a microwave-assisted method. Environmental Science and Pollution Research, 2016, 23, 4489-4497.	5.3	162
4	Removal of heavy metal ions from aqueous solution by zeolite synthesized from fly ash. Environmental Science and Pollution Research, 2016, 23, 2778-2788.	5.3	160
5	Enhanced degradation of triclosan by cobalt manganese spinel-type oxide activated peroxymonosulfate oxidation process via sulfate radicals and singlet oxygen: Mechanisms and intermediates identification. Science of the Total Environment, 2020, 711, 134715.	8.0	126
6	Simultaneous nitrification and denitrification without nitrite accumulation by a novel isolated Ochrobactrum anthropic LJ81. Bioresource Technology, 2019, 272, 442-450.	9.6	116
7	Ru–Ru ₂ PΦNPC and NPC@RuO ₂ Synthesized via Environmentâ€Friendly and Solidâ€Phase Phosphating Process by Saccharomycetes as N/P Sources and Carbon Template for Overall Water Splitting in Acid Electrolyte. Advanced Functional Materials, 2019, 29, 1901154.	14.9	112
8	The occurrence and abundance of microplastics in surface water and sediment of the West River downstream, in the south of China. Science of the Total Environment, 2021, 756, 143857.	8.0	102
9	Recovery of phosphorus and nitrogen from alkaline hydrolysis supernatant of excess sludge by magnesium ammonium phosphate. Bioresource Technology, 2014, 166, 1-8.	9.6	95
10	Simultaneous degradation of tetracycline and denitrification by a novel bacterium, Klebsiella sp. SQY5. Chemosphere, 2018, 209, 35-43.	8.2	92
11	Removal of tetracycline and oxytetracycline from water by magnetic Fe3O4@graphene. Environmental Science and Pollution Research, 2017, 24, 2987-2995.	5.3	84
12	Intra/extracellular electron transfer for aerobic denitrification mediated by in-situ biosynthesis palladium nanoparticles. Water Research, 2021, 189, 116612.	11.3	72
13	Distribution and characteristics of microplastics in the basin of Chishui River in Renhuai, China. Science of the Total Environment, 2021, 773, 145591.	8.0	71
14	Bacterial effects and interfacial inactivation mechanism of nZVI/Pd on Pseudomonas putida strain. Water Research, 2017, 115, 297-308.	11.3	69
15	Sorption/desorption behavior of triclosan in sediment–water–rhamnolipid systems: Effects of pH, ionic strength, and DOM. Journal of Hazardous Materials, 2015, 297, 59-65.	12.4	66
16	Biodegradation of oxytetracycline and electricity generation in microbial fuel cell with in situ dual graphene modified bioelectrode. Bioresource Technology, 2018, 270, 482-488.	9.6	65
17	High mesoporosity phosphorus-containing biochar fabricated from Camellia oleifera shells: Impressive tetracycline adsorption performance and promotion of pyrophosphate-like surface functional groups (C-O-P bond). Bioresource Technology, 2021, 329, 124922.	9.6	63
18	Filtration and Electrochemical Disinfection Performance of PAN/PANI/AgNWs-CC Composite Nanofiber Membrane. Environmental Science & Technology, 2017, 51, 6395-6403.	10.0	62

#	Article	IF	CITATIONS
19	Biodegradation mechanism of tetracycline (TEC) by strain Klebsiellaâ€,sp. SQY5 as revealed through products analysis and genomics. Ecotoxicology and Environmental Safety, 2019, 185, 109676.	6.0	56
20	Immobilization of laccase onto meso-MIL-53(Al) via physical adsorption for the catalytic conversion of triclosan. Ecotoxicology and Environmental Safety, 2019, 184, 109670.	6.0	55
21	Ultrafast Nanofiltration through Large-Area Single-Layered Graphene Membranes. ACS Applied Materials & Interfaces, 2017, 9, 9239-9244.	8.0	54
22	Bacterial community shift and improved performance induced by in situ preparing dual graphene modified bioelectrode in microbial fuel cell. Bioresource Technology, 2017, 238, 273-280.	9.6	53
23	Bacterial community shift and incurred performance in response to in situ microbial self-assembly graphene and polarity reversion in microbial fuel cell. Bioresource Technology, 2017, 241, 220-227.	9.6	50
24	Sequential decolorization of azo dye and mineralization of decolorization liquid coupled with bioelectricity generation using a pH self-neutralized photobioelectrochemical system operated with polarity reversion. Journal of Hazardous Materials, 2015, 289, 108-117.	12.4	49
25	Enhanced adsorption performance of MoS2 nanosheet-coated MIL-101 hybrids for the removal of aqueous rhodamine B. Journal of Colloid and Interface Science, 2017, 504, 39-47.	9.4	49
26	Carbon selection for nitrogen degradation pathway by Stenotrophomonas maltophilia: Based on the balances of nitrogen, carbon and electron. Bioresource Technology, 2019, 294, 122114.	9.6	48
27	Micro/macrostructure and multicomponent design of catalysts by MOF-derived strategy: Opportunities for the application of nanomaterials-based advanced oxidation processes in wastewater treatment. Science of the Total Environment, 2022, 804, 150096.	8.0	47
28	Adsorption of Cu ²⁺ and Cd ²⁺ from aqueous solution by novel electrospun poly(vinyl alcohol)/graphene oxide nanofibers. RSC Advances, 2016, 6, 79641-79650.	3.6	45
29	Action of oxytetracycline (OTC) degrading bacterium and its application in Moving Bed Biofilm Reactor (MBBR) for aquaculture wastewater pre-treatment. Ecotoxicology and Environmental Safety, 2019, 171, 833-842.	6.0	45
30	Effects of various antibiotics on aerobic nitrogen removal and antibiotic degradation performance: Mechanism, degradation pathways, and microbial community evolution. Journal of Hazardous Materials, 2022, 422, 126818.	12.4	45
31	Enhanced performance of microbial fuel cell with in situ preparing dual graphene modified bioelectrode. Bioresource Technology, 2017, 241, 735-742.	9.6	43
32	Synergistic effects in iron-copper bimetal doped mesoporous Î ³ -Al2O3 for Fenton-like oxidation of 4-chlorophenol: Structure, composition, electrochemical behaviors and catalytic performance. Chemosphere, 2018, 203, 442-449.	8.2	42
33	Application of a heavy metal-resistant Achromobacter sp. for the simultaneous immobilization of cadmium and degradation of sulfamethoxazole from wastewater. Journal of Hazardous Materials, 2021, 402, 124032.	12.4	41
34	Simultaneous sulfamethoxazole biodegradation and nitrogen conversion by Achromobacter sp. JL9 using with different carbon and nitrogen sources. Bioresource Technology, 2019, 293, 122061.	9.6	40
35	Effectively enhanced photodegradation of Bisphenol A by in-situ g-C3N4-Zn/Bi2WO6 heterojunctions and mechanism study. Chemosphere, 2020, 246, 125782.	8.2	40
36	Rhamnolipid-enhanced aerobic biodegradation of triclosan (TCS) by indigenous microorganisms in water-sediment systems. Science of the Total Environment, 2016, 571, 1304-1311.	8.0	38

#	Article	IF	CITATIONS
37	Effects of carbon source, nitrogen source, and natural algal powder-derived carbon source on biodegradation of tetracycline (TEC). Bioresource Technology, 2019, 288, 121567.	9.6	37
38	Bioaugmentation of Moving Bed Biofilm Reactor (MBBR) with Achromobacter JL9 for enhanced sulfamethoxazole (SMX) degradation in aquaculture wastewater. Ecotoxicology and Environmental Safety, 2021, 207, 111258.	6.0	37
39	Treatment of Ni-EDTA containing wastewater by electrocoagulation using iron scraps packed-bed anode. Chemosphere, 2016, 164, 304-313.	8.2	36
40	Simultaneous Cr(VI) reduction and electricity generation in Plant-Sediment Microbial Fuel Cells (P-SMFCs): Synthesis of non-bonding Co3O4 nanowires onto cathodes. Environmental Pollution, 2019, 247, 647-657.	7.5	35
41	Silver nanowire-carbon fiber cloth nanocomposites synthesized by UV curing adhesive for electrochemical point-of-use water disinfection. Chemosphere, 2016, 154, 537-545.	8.2	34
42	Simultaneous sulfamethoxazole biodegradation and nitrogen conversion in low C/N ratio pharmaceutical wastewater by Achromobacter sp. JL9. Science of the Total Environment, 2020, 703, 135586.	8.0	34
43	Water Quality and Microbial Community Changes in an Urban River after Micro-Nano Bubble Technology in Situ Treatment. Water (Switzerland), 2019, 11, 66.	2.7	33
44	Effects of an organic carbon source on the coupling of sulfur(thiosulfate)-driven denitration with Anammox process. Bioresource Technology, 2021, 335, 125280.	9.6	31
45	Interaction among multiple microorganisms and effects of nitrogen and carbon supplementations on lignin degradation. Bioresource Technology, 2014, 155, 144-151.	9.6	30
46	Enhanced performance of sulfamethoxazole degradation using Achromobacter sp. JL9 with in-situ generated biogenic manganese oxides. Bioresource Technology, 2021, 333, 125089.	9.6	30
47	Enhanced degradation of diclofenac with Ru/Fe modified anode microbial fuel cell: Kinetics, pathways and mechanisms. Bioresource Technology, 2020, 300, 122703.	9.6	29
48	Effect of calcination temperature on the properties of Ti/SnO2-Sb anode and its performance in Ni-EDTA electrochemical degradation. Environmental Science and Pollution Research, 2018, 25, 11683-11693.	5.3	28
49	Comparison of Different Enhanced Coagulation Methods for Azo Dye Removal from Wastewater. Sustainability, 2019, 11, 4760.	3.2	28
50	Impact of microwave power on the preparation of silver nanowires via a microwave-assisted method. RSC Advances, 2013, 3, 8431.	3.6	26
51	Novel AgNWs-PAN/TPU membrane for point-of-use drinking water electrochemical disinfection. Science of the Total Environment, 2018, 637-638, 408-417.	8.0	26
52	The effects of Fe2+ on sulfur-oxidizing bacteria (SOB) driven autotrophic denitriffation. Journal of Hazardous Materials, 2019, 373, 359-366.	12.4	26
53	SWNTs-PAN/TPU/PANI composite electrospun nanofiber membrane for point-of-use efficient electrochemical disinfection: New strategy of CNT disinfection. Chemosphere, 2020, 251, 126286.	8.2	26
54	In-situ fabrication of ionic liquids/MIL-68(In)–NH2 photocatalyst for improving visible-light photocatalytic degradation of doxycycline hydrochloride. Chemosphere, 2022, 292, 133461.	8.2	25

#	Article	IF	CITATIONS
55	Electron transfer involved in bio-Pd (0) synthesis by Citrobacter freundii at different growth phases. Ecotoxicology and Environmental Safety, 2020, 190, 110124.	6.0	20
56	Screening pretreatment methods for sludge disintegration to selectively reclaim carbon source from surplus activated sludge. Chemical Engineering Journal, 2014, 255, 365-371.	12.7	19
57	Synthesis of SiO ₂ coated zero-valent iron/palladium bimetallic nanoparticles and their application in a nano-biological combined system for 2,2′,4,4′-tetrabromodiphenyl ether degradation. RSC Advances, 2016, 6, 20357-20365.	3.6	18
58	Co-N-doped MoO2 modified carbon felt cathode for removal of EDTA-Ni in electro-Fenton process. Environmental Science and Pollution Research, 2018, 25, 22754-22765.	5.3	18
59	Positive effects of bio-nano Pd (0) toward direct electron transfer in Pseudomona putida and phenol biodegradation. Ecotoxicology and Environmental Safety, 2018, 161, 356-363.	6.0	18
60	Decomplexation efficiency and mechanism of Cu(II)–EDTA by H2O2 coupled internal micro-electrolysis process. Environmental Science and Pollution Research, 2019, 26, 1015-1025.	5.3	18
61	Prompting direct single electron transfer to produce non-radical 102/H* by electro-activating peroxydisulfate process with core-shell cathode. Journal of Environmental Management, 2021, 287, 112294.	7.8	17
62	Simultaneous mineralization of 2-anilinophenylacetate and denitrification by Ru/Fe modified biocathode double-chamber microbial fuel cell. Science of the Total Environment, 2021, 792, 148446.	8.0	17
63	Highly efficient catalytic ozonation for ammonium in water upon γ-Al2O3@Fe/Mg with acidic-basic sites and oxygen vacancies. Science of the Total Environment, 2022, 834, 155278.	8.0	17
64	Prompting the FDH/Hases-based electron transfers during Pt(IV) reduction mediated by bio-Pd(0). Journal of Hazardous Materials, 2021, 417, 126090.	12.4	16
65	Biofilm evolution and viability during in situ preparation of a graphene/exoelectrogen composite biofilm electrode for a high-performance microbial fuel cell. RSC Advances, 2017, 7, 42172-42179.	3.6	16
66	Activation of Oxytetracycline Extracellular Degradation in <i>Bacillus megaterium</i> : Outward Transmembrane Electron Transfer and Energy Metabolism via Bio-Pd ⁰ Nanoparticles. ACS ES&T Water, 2021, 1, 2412-2422.	4.6	15
67	Enhanced selection of micro-aerobic pentachlorophenol degrading granular sludge. Journal of Hazardous Materials, 2014, 280, 134-142.	12.4	14
68	Enhanced denitrification of sewage via bio-microcapsules embedding heterotrophic nitrification-aerobic denitrification bacteria Acinetobacter pittii SY9 and corn cob. Bioresource Technology, 2022, 358, 127260.	9.6	13
69	Degradation of diclofenac via sequential reduction-oxidation by Ru/Fe modified biocathode dual-chamber bioelectrochemical system: Performance, pathways and degradation mechanisms. Chemosphere, 2022, 291, 132881.	8.2	12
70	Selective removal and preconcentration of triclosan using a water-compatible imprinted nano-magnetic chitosan particles. Environmental Science and Pollution Research, 2017, 24, 18640-18650.	5.3	11
71	Biomineralization of 2′2′4′4′-Tetrabromodiphenyl ether in a Pseudomonas putida and Fe/Pd nanoparti integrated system. Chemosphere, 2019, 221, 301-313.	cles 8.2	11
72	Simultaneous separation and determination of seven chelating agents using highâ€performance liquid chromatography based on statistics design. Journal of Separation Science, 2020, 43, 719-726.	2.5	11

#	Article	IF	CITATIONS
73	Sulfidation forwarding high-strength Anammox process using nitrate as electron acceptor via thiosulfate-driven nitrate denitratation. Bioresource Technology, 2022, 344, 126335.	9.6	11
74	Enhanced Ozone Oxidation by a Novel Fe/Mn@î³â^'Al2O3 Nanocatalyst: The Role of Hydroxyl Radical and Singlet Oxygen. Water (Switzerland), 2022, 14, 19.	2.7	10
75	Oxytetracycline co-metabolism with denitrification/desulfurization in SRB mediated system. Chemosphere, 2022, 298, 134256.	8.2	9
76	Pd/RGO modified carbon felt cathode for electro-Fenton removing of EDTA-Ni. Water Science and Technology, 2016, 74, 639-646.	2.5	7
77	Experimental investigation on the water stability of amino-modified indium metal–organic frameworks. RSC Advances, 2016, 6, 61703-61706.	3.6	7
78	Synthesis, characterization, and debromination reactivity of cellulose-stabilized Pd/Fe nanoparticles for 2,2',4,4'-tretrabromodiphenyl ether. PLoS ONE, 2017, 12, e0174589.	2.5	7
79	Electro-activating non-radical 1O2/H*Âvia single atom manganese modified cathode: The indispensable role of metal active site Mn*. Journal of Hazardous Materials, 2022, 426, 127794.	12.4	6
80	Effect of cations on the solubilization/deposition of triclosan in sediment-water-rhamnolipid system. Chemosphere, 2016, 159, 465-472.	8.2	4
81	Investigation of the accumulation of ash, heavy metals, and polycyclic aromatic hydrocarbons to assess the stability of lysis–cryptic growth sludge reduction in sequencing batch reactor. Environmental Science and Pollution Research, 2017, 24, 24147-24155.	5.3	4
82	Conversion Mechanisms of Carbon, Nitrogen, and Phosphorus in Ozone-Fixed-Bed and Membrane Bioreactors for Deep Treatment of Municipal Tail Water. Environmental Engineering Science, 2017, 34, 562-568.	1.6	3
83	CFD simulation of a swirling vortex cavitator and its degradation performance and pathway of tetracycline in aqueous solution. International Journal of Chemical Reactor Engineering, 2022, 20, 955-963.	1.1	3
84	Dissolving organic matter from low-organic sewage sludge for shortening the anaerobic digestion time. RSC Advances, 2018, 8, 36951-36958.	3.6	2
85	Catalytic Reduction of Nitrate by Pd/SnO2 Catalyst Using Formic Acid as Reducing Agent. International Conference on Bioinformatics and Biomedical Engineering: [proceedings] International Conference on Bioinformatics and Biomedical Engineering, 2010, , .	0.0	1
86	Direct growth of a porous substrate on high-quality graphene <i>via in situ</i> phase inversion of a polymeric solution. Nanoscale, 2020, 12, 4953-4958.	5.6	1
87	Effects of Probiotic Fermented Kitchen Waste on the Growth and Propagation of Rotifer <i>Brachionus calyciflorus</i> . Journal of Biobased Materials and Bioenergy, 2021, 15, 83-89.	0.3	1
88	Enhancing Phosphorus Recovery and Dewaterability of Waste Activated Sludge for Combined Effect of Thermally Activated Peroxydisulfate and Struvite Precipitation. Sustainability, 2021, 13, 9700.	3.2	1
89	Production of a Novel Bioflocculant by Culture of Penicillium purpurogenum HHE-P7 Using Confectionery Wastewater. International Conference on Bioinformatics and Biomedical Engineering: [proceedings] International Conference on Bioinformatics and Biomedical Engineering, 2010, , .	0.0	0